Quantum Monte Carlo calculations of H_2 dissociation on Si(001)

Claudia Filippi[1], Sorcha B. Healy[2], P. Kratzer[3], E. Pehlke[4], and M. Scheffler[3]
[1] *Universiteit Leiden, Instituut Lorentz, Niels Bohrweg 2, Leiden, NL-2333 CA, The Netherlands*
[2] *Physics Department, National University of Ireland, Cork, Ireland*
[3] *Fritz-Haber-Institut der Max-Planck-Gesellschaft, Faradayweg 4-6, D-14195 Berlin-Dahlem, Germany*
[4] *Institut für Laser und Plasmaphysik, Universität Essen, 45117 Essen, Germany*
(February 1, 2008)

We present quantum Monte Carlo calculations for various reaction pathways of H_2 with Si(001), using large model clusters of the surface. We obtain reaction energies and energy barriers noticeably higher than those from approximate exchange-correlation functionals. In improvement over previous studies, our adsorption barriers closely agree with experimental data. For desorption, the calculations give barriers for conventional pathways in excess of the presently accepted experimental value, and pinpoint the role of coverage effects and desorption from steps.

The dissociative adsorption of molecular hydrogen on the Si(001) surface has become a paradigm in the study of adsorption systems. Despite its apparent simplicity, more than a decade of extensive experimental and theoretical investigations have not clarified fundamental aspects of the chemical reaction of H_2 with this surface.

Many of the experimental observations are hard to reconcile in a unified picture: the sticking probability for dissociative adsorption of H_2 on the clean surface is very small at room temperature suggesting a high adsorption barrier; sticking increases dramatically with higher surface temperatures [1]. On the other hand, the nearly thermally distributed kinetic energy of desorbing molecules has lead researchers to the conclusion that the molecules have transversed almost no adsorption barrier [2]. Microscopically, these observations were originally interpreted in terms of an intra-dimer mechanism, where the hydrogen molecule interacts with one single dimer of the Si(001) surface [3]. However, very recent experiments have pointed to additional mechanisms involving not just a single dimer but nearby dimers [4,5]. The existence of highly reactive pathways was first demonstrated on steps [6] or H-precovered surfaces [7], and evidence that H_2 reacts with two adjacent dimers has also now been given for the clean surface [8]. In Fig. 1, the intra-dimer (H2*) and two inter-dimer pathways at different coverages (H2 and H4) are schematically shown.

Theoretically, density-functional theory (DFT) calculations performed on intra-dimer and inter-dimer mechanisms have lead to limited agreement with experiments. While correctly predicting the existence of a barrier-less H4 inter-dimer reaction path at high coverages [9], previous DFT slab calculations yielded an adsorption barrier for the low-coverage H2* and H2 pathways too low to explain the small sticking coefficient observed at low temperatures [7]. Desorption barriers from DFT obtained within the generalized gradient approximation (GGA) were also generally lower than the experimental value (2.5 eV, Ref. [10]). Additional evidence for a possible inadequacy of DFT-GGA to describe this reaction comes from comparison with highly correlated quantum chemistry calculations for small cluster models of the surface: For the intra-dimer pathway, these methods obtain values for the desorption barrier that are at large variance with the DFT-GGA value [11–13].

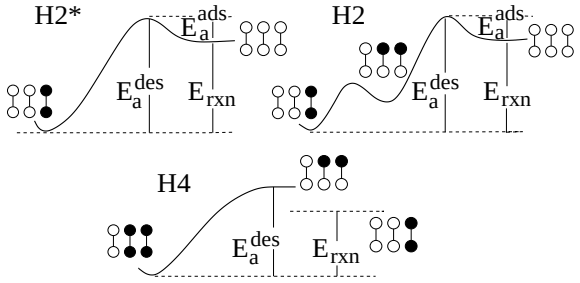

FIG. 1. Intra-dimer (H2*) and inter-dimer mechanisms at low (H2) and high (H4) coverages. The surface configuration along the pathway is schematically shown: A circle represents a Si atom and a filled circle Si–H. E_a^{ads}, E_a^{des} and E_{rxn} are the adsorption, desorption and reaction energies, respectively.

In this Letter, we use quantum Monte Carlo (QMC) techniques on large cluster models of the surface to accurately compute the reaction energetics of H_2 on Si(001) for the intra-dimer and inter-dimer mechanisms, as well as adsorption at steps. The reliability of a calculation depends both on the level of theory at which electronic correlations are treated, as well as on the geometrical model used to describe the system. Compared to other theoretical approaches, QMC offers the advantage that accurate reaction energetics can be computed for relatively large systems. Our calculations predict reaction energies and barriers noticeably higher than those obtained in DFT with the local density approximation or commonly used GGAs. Even though distinctly lower, the energetics determined with the B3LYP [14] hybrid functional are the only ones in fair agreement with the QMC results. When compared to experiments, the QMC ad-

TABLE I. Adsorption (E_a^{ads}), desorption (E_a^{des}) and reaction (E_{rxn}) energies in eV for H_2/Si(001) via the intra-dimer H2* mechanism (see Fig. 1), calculated within PW91, B3LYP and QMC. Zero-point energies (ZPE) are not included.

	PW91			B3LYP			QMC		
	E_a^{ads}	E_a^{des}	E_{rxn}	E_a^{ads}	E_a^{des}	E_{rxn}	E_a^{ads}	E_a^{des}	E_{rxn}
Si_9H_{12}	0.69	2.86	2.17	0.90	3.40	2.50	1.01±0.06	3.65±0.06	2.64±0.06
$Si_{15}H_{16}$	0.56	2.65	2.09	0.71	3.20	2.49	0.98±0.05	3.52±0.07	2.54±0.06
$Si_{21}H_{20}$	0.32	2.31	1.99	0.56	2.90	2.35	0.61±0.05	3.11±0.05	2.49±0.05
$Si_{27}H_{24}$	0.37	2.35	1.98	0.57	2.91	2.33	0.49±0.13	3.03±0.13	2.54±0.13

sorption barriers for the intra-dimer (H2*) and the low-coverage inter-dimer (H2) pathways can explain why the sticking coefficient on the clean Si(001) surface is so small at low temperatures. Moreover, the QMC desorption barriers represent an important input for the interpretation of experimental results.

Computational methods. We employ slabs as well as clusters to mimic the Si(001) surface. The surface can be appropriately modeled with clusters containing only a single row of dimers [15]: interactions are negligible between neighboring dimer rows, while substantial between dimers in the same row. Such clusters with one, two, three, and four dimers are Si_9H_{12}, $Si_{15}H_{16}$, $Si_{21}H_{20}$, and $Si_{27}H_{24}$. They represent a four layer cut of the Si(001) surface with all but the surface atoms terminated with hydrogens to passivate dangling bonds. Two separate clusters are constructed to model the clean surface and the surface after adsorption of a hydrogen molecule; the transition state (TS) connecting the the two configurations is then determined.

As a starting point, plane-wave pseudopotential calculations within DFT were performed to obtain geometries and total energies of both the cluster and slab models. For details on the construction and the geometry of the clusters, see Ref. [16]. We optimized all geometries using the PW91 functional [17], which gives a good description of the structural properties of Si (lattice constant error $< 1\%$). Moreover, for cluster models of H_2/Si(001), the geometries optimized using PW91 and the hybrid functional B3LYP were found to be very similar [18], and the energetics of the reaction on both sets of geometries essentially the same within B3LYP (as shown below, B3LYP gives energies very close to our accurate QMC results). It is therefore a sound procedure to use QMC on geometries obtained from PW91 calculations to assess whether a more accurate treatment of electronic correlation can change the physical picture.

We calculate the energetics for various reaction pathways of H_2 on the Si(001) using B3LYP and QMC for the cluster geometries, and PW91 for both clusters and slab. The many-body wave function used in QMC is of the form given in Ref. [19] (modified to deal with pseudoatoms):

$$\Psi = \sum_n d_n D_n^{\uparrow} D_n^{\downarrow} \prod_{\alpha ij} J\left(r_{ij}, r_{i\alpha}, r_{j\alpha}\right) .$$

$D_n^{\uparrow}$ and $D_n^{\downarrow}$ are Slater determinants of single particle orbitals for the up and down electrons, respectively, and the orbitals are represented using atomic Gaussian basis [20]. The Jastrow factor correlates pairs of electrons i and j with each other, and with every nucleus α, and different Jastrow factors are used to describe the correlation with a hydrogen and a silicon atom. The determinantal part of the wave function is generated within Hartree-Fock or MCSCF, using the quantum chemistry package GAMESS [21]. The parameters in the Jastrow factor are optimized within QMC using the variance minimization method [22] and the accuracy of the wave function tested at the variational level. The wave function is then used in diffusion Monte Carlo (DMC), which produces the best energy within the fixed-node approximation (i.e. the lowest-energy state with the same nodes as the trial wave function) [23]. All QMC results presented are from DMC calculations.

Intra-dimer mechanism. In the H2* pathway, the hydrogen molecule dissociatively adsorbs on the same Si dimer through an asymmetric TS. Multi-reference configuration interaction (MRCI) calculations [13] on Si_9H_{12} yield adsorption and desorption barriers which are 0.3 and 0.8 eV higher than the corresponding PW91 values listed in Table I. Given the magnitude of the discrepancy, it is important to ascertain whether this difference will persist in going from the one-dimer model to a more realistic representation of the surface. QMC gives energies in very good agreement with the MRCI results for Si_9H_{12} and, unlike traditional quantum chemistry methods, can be applied to larger models of the surface to study the convergence of the reaction energies with cluster size and access accurate estimates for the real surface.

In Table I, we list the PW91, B3LYP and QMC adsorption, desorption and reaction energies via the intra-dimer mechanism for the clusters with one, two, three, and four surface dimers. The QMC energies are consistently higher than the PW91 values for all clusters: The QMC adsorption, desorption and reaction energies are above the PW91 values by about 0.3, 0.8 and 0.5 eV, respectively. Therefore, the corrections to the PW91 values due to the incorrect treatment of electronic correlation are indeed significant, and, interestingly, they do not show a noticeable dependence on the size of the cluster. The QMC results for $Si_{27}H_{24}$ have a large errorbar but also demonstrate the smooth QMC convergence with system size. B3LYP represents a significant improvement upon PW91, giving energies which are much

closer to our QMC results, and only lower by about 0.05, 0.2, and 0.15 eV for $Si_{21}H_{20}$. This is in accordance with earlier studies using the B3LYP functional for the Si–H system [11,18,24].

TABLE II. Adsorption, desorption and reaction energies in eV per molecule for H_2/Si(001) via the H2 and H4 mechanisms (see Fig. 1). The $Si_{27}H_{24}$ model cluster of the surface is used.

	E_a^{ads}	E_a^{des}	E_{rxn}
H2 mechanism			
PW91	0.26	2.24	1.99
B3LYP	0.54	2.87	2.33
QMC	0.59±0.09	3.11±0.09	2.52±0.09
H4 mechanism			
PW91	0.00	2.46	2.13
B3LYP	0.00	2.91	2.50
QMC	0.19±0.14	3.18±0.12	2.61±0.11

Inter-dimer H2 and H4 mechanisms. In the H2 pathway, the hydrogen molecule dissociates over two clean neighboring Si dimers, yielding a cis configuration with two hydrogens bound to two Si atoms at the same side of the dimers. For the H4 mechanism, the adsorption occurs on two neighboring Si dimers which are both already covered on the same side with hydrogens (see Fig. 1). The configuration after adsorption consists of two fully covered Si dimers. The PW91, B3LYP and QMC adsorption, desorption and reaction energies for the H2 and H4 pathways are presented in Table II. All calculations were performed on the four-dimer cluster $Si_{27}H_{24}$ and the reaction occurs on the two central dimers. For both mechanisms, the results show the same trends as for the intra-dimer pathway: PW91 significantly underestimates reaction energies and barriers, and B3LYP is much closer to the QMC results than PW91. For the H4 mechanism, PW91 and B3LYP predict no adsorption barrier. Within the statistical error, we find this to remain true also in the QMC calculation. To explore a possible QMC adsorption barrier, we computed the QMC energies for nine geometries along the path connecting the configuration of four hydrogens on two neighboring dimers with the configuration of two hydrogens in the cis configuration plus a desorbed hydrogen molecule. However, the cis configuration does *not* constitute the energetically lowest adsorption geometry of two hydrogens atoms, and thus occurs only scarcely. The pairing energy, that is the energy difference between the cis configuration and two hydrogens at the same Si dimer, is found to be 0.34, 0.42 and 0.54±0.07 eV in PW91, B3LYP and QMC, respectively [25].

Discussion and conclusions. In addition to accessing the reliability of approximate DFT in describing H-Si bonded systems, we can use our accurate QMC energetics to understand the physics of the interaction of hydrogen with the Si(001) surface. In order to compare with the available experimental results for the H_2/Si(001) system, we need to extrapolate the QMC energies to the infinite-system limit and include the zero-point energy corrections (ΔZPE). To compute the extrapolated QMC results, we start from the PW91 infinite-system limit, that is the PW91 slab energy, and add a correction for the inaccurate treatment of electronic exchange and correlation estimated from the cluster calculation as $\Delta E_{corr} = E^{QMC}_{cluster} - E^{PW91}_{cluster}$. After including the ZPE contribution, the final QMC energy is $E^{QMC} = E^{PW91}_{slab} + (E^{QMC}_{cluster} - E^{PW91}_{cluster}) + \Delta ZPE$. In Table III, the extrapolated QMC energies are compared with the experimental results.

TABLE III. Extrapolated QMC adsorption, desorption and reaction energies in eV for the H2*, H2 and H4 mechanisms (see text). [a]Ref. [18] (identical ΔZPE assumed for all mechanisms); [b]Ref. [7]; [c]Ref. [10]; [d]Ref. [26].

	E_a^{ads}	E_a^{des}	E_{rxn}
H2* mechanism			
E^{PW91}_{slab}	0.37	2.27	1.90
ΔZPE^a	+0.09	−0.11	−0.20
ΔE_{corr}	+0.29±0.05	+0.80±0.05	+0.50±0.05
E^{QMC}	0.75±0.05	2.96±0.05	2.20±0.05
Expt.	>0.6[b]	2.5±0.1[c]	1.9±0.3[d]
H2 mechanism			
E^{PW91}_{slab}	0.20	2.15	1.95
ΔZPE^a	+0.09	−0.11	−0.20
ΔE_{corr}	+0.34±0.09	+0.87±0.09	+0.53±0.09
E^{QMC}	0.63±0.09	2.91±0.09	2.28±0.09
Expt.	>0.6[b]	2.5±0.1[c]	1.9±0.3[d]
H4 mechanism			
E^{PW91}_{slab}	0.00	2.32	2.01
ΔZPE^a	N/A	−0.20	−0.20
ΔE_{corr}	+0.19±0.14	+0.72±0.12	+0.48±0.11
E^{QMC}	0.19±0.14	2.84±0.12	2.29±0.11
Expt.	0.00[b]	2.5±0.1[c]	N/A

The PW91 slab reaction energies and barriers are significantly lower than the experimental results and, for E_a^{des} and E_{rxn}, the discrepancy is even amplified when the negative ZPE's are added. As discussed above, the QMC energetics for the clusters are higher than the corresponding PW91 values for all the mechanisms, so the correlation corrections are positive and the extrapolated QMC results significantly higher than the original PW91 slab energies. The final reaction energies are compatible with experiments and the adsorption barriers are in much better agreement with the experimental results than the PW91 barriers. The larger adsorption barriers for the intra-dimer and the low-coverage H2 inter-dimer pathways can finally explain why the sticking coefficient on the clean Si(001) surface is so small at low temperatures. Moreover, the high reactivity for adsorption via the H4 mechanism is corroborated by the QMC results

which are consistent with a barrier-less pathway. Possibly, the dramatic increase in sticking probability with surface temperature is partly due to this pathway: if hydrogen is already present on the surface, an increase in surface temperature leads to an increased number of cis configurations, thus creating barrier-less adsorption sites for sticking.

Concerning desorption, the picture is more complicated. Judging from the extrapolated QMC barriers, none of the studied mechanisms appears to be compatible with the desorption energy of 2.5±0.1 eV observed in temperature-programmed desorption experiments [10]. However, such experiments could have been affected by a small concentration of surface imperfections. To exemplify this possibility, we looked at the adsorption/desorption of H_2 at the D_B step edge which is modeled as a $Si_{28}H_{28}$ cluster constructed from previous slab calculations [6]. Experimentally, a small adsorption barrier of 0.09±0.01 eV is observed while PW91 predicts no adsorption barrier, so PW91 desorption and reaction energies are the same. Here, we compute only the B3LYP and QMC reaction energies for $Si_{28}H_{28}$, which are equal to 2.54 and 2.81±0.07 eV, respectively. The extrapolated QMC value is 2.61±0.07 eV, significantly lower than the other desorption barriers, and hence the presence of a small number of steps could dominate the desorption yield. Our calculations suggest that the hitherto accepted experimental value of the desorption barrier should be referred to desorption from steps or defects, rather than to one of the mechanisms discussed for ideal Si(001) surfaces. For experiments where contributions from surface imperfections are carefully avoided (e.g. by heating the surface only very locally), the QMC calculations predict a slight preference for the H4 mechanism. While the lack of an adsorption barrier along the H4 pathway can explain the low kinetic energy of the desorbing hydrogen molecules, one should also keep in mind the observed vibrational excitation in desorption [27], indicating that some molecules desorb on a pathway with an adsorption barrier. We conclude that several mechanisms contribute to desorption, whose relative importance depends sensitively on temperature, coverage, and surface perfection.

In this Letter, we presented accurate QMC calculations for various pathways of adsorption/desorption of H_2 from Si(001), using large cluster models of the surface. For intra-dimer and inter-dimer pathways, we find that PW91 significantly underestimates reaction energies and barriers, while B3LYP yields energetics in much better agreement with the QMC values. Caution should therefore be used when employing PW91 or other GGAs in the study of Si–H systems. Finally, the QMC adsorption barriers are in close agreement with experimental values while the results for desorption call for further experimental studies of the activation energy and its dependence on coverage and surface perfection.

[1] M. Dürr, M. B. Raschke, and U. Höfer, J. Chem. Phys. **111**, 10411 (1999).
[2] K. W. Kolasinski *et al.*, Phys. Rev. Lett. **62**, 1356 (1994).
[3] E. Pehlke and M. Scheffler, Phys. Rev. Lett. **74**, 952 (1995). P. Kratzer, B. Hammer, and J. K. Nørskov, Phys. Rev. B **51**, 13432 (1996); A. Gross, M. Bockstedte, and M. Scheffler, **79**, 701 (1997).
[4] F. M. Zimmermann and X. Pan, Phys. Rev. Lett. **85**, 618 (2000).
[5] A. Biedermann *et al.*, Phys. Rev. Lett. **83**, 1810 (2001).
[6] P. Kratzer *et al.*, Phys. Rev. Lett. **81**, 5596 (1998).
[7] M. Dürr *et al.*, Phys. Rev. Lett. **86**, 123 (2001).
[8] M. Dürr *et al.*, Phys. Rev. Lett. **88**, 046104 (2002).
[9] E. Pehlke, Phys. Rev. B **62**, 12932 (2000).
[10] U. Höfer, L. Li, and T. F. Heinz, Phys. Rev. B **45**, R9485 (1992).
[11] P. Nachtigall *et al.*, J. Chem. Phys. **104**, 148 (1996).
[12] M. R. Radeke and E. A. Carter, Phys. Rev. B **54**, 11803 (1996).
[13] Z. Jing and J. L. Whitten, J. Chem. Phys. **98**, 7466 (1993); *ibid.* **102**, 3867 (1995).
[14] A. D. Becke, J. Chem. Phys. **98**, 5648 (1993); C. Lee, W. Yang, and R. G. Parr, Phys. Rev. B **37**, 785 (1988).
[15] S. B. Healy *et al.* Phys. Rev. Lett. **87**, 016105 (2001).
[16] E. Penev, P. Kratzer, and M. Scheffler, J. Chem. Phys. **110**, 3986 (1999); in improvement over this work, transition states were re-optimized, and energies calculated for a plane-wave basis set with a cut-off up to 40 Ry.
[17] J. P. Perdew in *Electronic structure of solids '91*, edited by P. Ziesche and H. Eschrig (Akademie Verlag, Berlin, 1991).
[18] J. A. Steckel *et al.*, J. Phys. Chem. B **105**, 4031 (2001); in Table 4, the angles for the geometries optimized in B3LYP are 3.3, 12.6 and 13.1 deg for reactant, TS and product, respectively.
[19] C. Filippi and C. J. Umrigar, J. Chem. Phys. **105**, 213 (1996).
[20] The Gaussian basis sets are $(10s10p1d)/[3s3p1d]$ for silicon and $(10s1p)/[3s1p]$ for hydrogen, and are optimized at the HF level for the Si_9H_{12} cluster.
[21] M. W. Schmidt *et al.*, J. Comput. Chem. **14**, 1347 (1993).
[22] C. J. Umrigar, K. G. Wilson, and J. W. Wilkins, Phys. Rev. Lett. **60**, 1719 (1988).
[23] P. J. Reynolds *et al.*, J. Chem. Phys. **77** 5593 (1982); L. Mitas, E. L. Shirley, and D. M. Ceperley, *ibid.* **95**, 3467 (1991); C. J. Umrigar, M. P. Nightingale, and K. J. Runge, *ibid.* **99**, 2865 (1993).
[24] Y. Okamoto, J. Phys. Chem. B **106**, 570 (2002).
[25] The PW91 slab value for the pairing energy is 0.31 eV.
[26] M. B. Raschke and U. Höfer, Phys. Rev. B **63**, R201303 (2001).
[27] K. W. Kolasinski, S. F. Shane, and R. N. Zare, J. Chem. Phys. **96**, 3995, (1992).